

## Model of mesons with constituent gluons\*

D. Horn<sup>†</sup>

*California Institute of Technology, Pasadena, California 91125*

J. Mandula<sup>‡</sup>

*Massachusetts Institute of Technology, Cambridge, Massachusetts 02139*

(Received 28 January 1977)

A model of mesons composed of a quark, an antiquark, and a gluon is proposed. The binding of the constituents is provided by a confining linear potential between the gluon and the quarks. The lowest states of the model are described, and their relative masses evaluated, for the case of heavy (charmed) quarks, i.e.,  $c\bar{c}g$  states.

### I. INTRODUCTION

A widespread approach to strong interactions views them as the realization of a color-symmetric gauge theory of quarks and gluons. The justification of this approach relies heavily on the fact that, through asymptotic freedom,<sup>1</sup> it can account for the high-energy experiments<sup>2</sup> which use currents as probes of hadronic dynamics. Recently this theory has been applied to the hadronic spectrum with notable success in charmonium models.<sup>3,4</sup> The role of the gluons in such models is to carry the force which attracts the quark to the antiquark, thus creating a binding, and supposedly confining, potential for the quark-antiquark system. It should be expected, though, that the quark-gluon field theory has a much richer meson spectrum than is describable by a quark and an antiquark in a confining potential. In fact, several authors have studied other systems, such as  $q\bar{q}q\bar{q}$ .<sup>5</sup> There too, the gluons serve merely as the carriers of the confining forces.

From the analysis of deep-inelastic electron scattering, we know that a major portion of the proton momentum is carried by neutral components which are customarily identified with gluons.<sup>2,6</sup> In this context, the gluons play a role which is analogous to that of the (current) quarks. In this paper we propose that the gluons may also play a role analogous to the (constituent) quarks in bound-state configurations. In particular, we study three-body bound states of a quark, an antiquark, and a gluon, where the force between the gluon and either the quark or the antiquark has the same confining nature as the force which binds quarks and antiquarks in ordinary mesons.

In a Yang-Mills theory,<sup>7</sup> the division of the gluon field into a part which represents quanta and a part which represents forces is well defined, although the breakup depends on the gauge. In the radiation gauge the division is especially natural.

There, the transverse part of the space components of the gluon field  $A_\mu^a$  represents quanta, while the time component is a dependent field representing an instantaneous potential between quanta.

Although we find it convenient to think about the bound states of a quark, an antiquark, and a gluon in a gauge-dependent way, we can associate them with the quanta created by gauge-invariant operators in the quark-gluon field theory. For example, the ground-state levels can be thought of as the quanta of the composite fields  $\bar{\psi}\gamma_\lambda\gamma_5 F_{\mu\lambda}\psi$  and  $\bar{\psi}\gamma_\nu\gamma_\lambda F_{\mu\lambda}\psi$ , which have the same quantum numbers as  $\bar{\psi}\gamma_5 D_\mu\psi$  and  $\bar{\psi}\gamma_\nu D_\mu\psi$  (where  $D_\mu$  is the gauge-invariant derivative), the operators associated with the  $L=1$   $q\bar{q}$  states of the quark model.

Some of the new quark-antiquark-gluon bound states have exotic quantum numbers, that is, they cannot couple to a fermion-antifermion system, but others have the same quantum numbers as states made just from a quark and an antiquark. While the exotics cannot be confused with ordinary  $q\bar{q}$  mesons, the others will presumably mix with conventional quark-model states. Nonetheless, the  $q\bar{q}g$  states represent new levels in addition to the  $q\bar{q}$  ones, thus increasing the total number of states with given quantum numbers. We find many new vector mesons which could contribute to the rich resonance structure observed in  $e^+e^-$  annihilation above 4 GeV.<sup>8</sup>

The organization of this paper is as follows:

In Sec. II we formulate an effective-potential model to describe three-body bound states involving a heavy (charmed) quark and antiquark and a massless gluon. We expect our Hamiltonian formalism to represent effects to order  $m_q^{-1}$ . Since octet-gluon exchange gives attractive quark-gluon and antiquark-gluon forces, we assume attractive potentials between these pairs of particles. Linear potentials have been successful in explaining the charmonium spectrum,<sup>3,4</sup> and we

take the attractive potentials in our model to be linear also. The parameters of the effective Hamiltonian are determined by comparison with charmonium calculations. The gluon-exchange strength is calculated in the Appendix.

In Sec. III we analyze the quantum numbers of the resulting bound states. The ground state is a set of levels with the same quantum numbers as those of the  $l=1$   $c\bar{c}$  states, and the first excited states contain, among others, three vector mesons as well as mesons with exotic  $J^{PC}$  quantum numbers. Table I contains a summary of the quantum numbers of states in the first few levels.

In Sec. IV we perform variational calculations of level splittings and conclude that the first excited levels will occur only about 300 MeV above the lowest levels. Our model does not fix the mass of the lowest  $c\bar{c}g$  state. However, since the states discussed here involve only a single massless quantum beyond  $c\bar{c}$ , they may well be the lightest mesons not included in the  $c\bar{c}$  sector, and include the lowest-mass exotic states.

We conclude with Sec. V, which contains a summary and discussion of our results.

## II. THE MODEL

Our model for quark-antiquark-gluon bound states is indirectly based on the colored quark-gluon model<sup>1</sup> and incorporates the linear effective potential of recent charmonium calculations.<sup>3,4</sup> We assume that the gluons have the quantum numbers attributed to them by the quark-gluon model, that they are color-octet and flavor-singlet massless vector mesons. We also assume that the forces between quarks and gluons are due to gluon exchange. Specifically, we assume that there are attractive forces in those channels in which color-octet-gluon exchange dictates it. Following the successful charmonium calculations, we represent these attractive forces by linear potentials.

We restrict our attention to states which are overall color singlets. The reason for this is that we expect that any nonsinglet configuration would have long-range interactions with others, and so could not be considered an isolated system.

We wish to represent this model by an effective Hamiltonian, but to do this we must specify a Lorentz frame. In order to have a dynamically preferred frame, we will assume that the quark mass is large, and express the Hamiltonian in the quark-antiquark center-of-mass frame. This choice limits the physical applicability of our results to bound states with charmed (or still heavier) quarks and antiquarks.

The effective Hamiltonian has kinetic-energy terms for each of the quarks and for the gluon,

effective  $r$  potentials, and an overall constant. Since the quarks are heavy and presumably slow-moving, we treat their energies nonrelativistically. This is an approximation to  $O(m_q^{-1})$ , and one may regard our spectral model as the leading term in an expansion in  $m_q^{-1}$ . By contrast the gluon is massless, and so its kinetic energy is the absolute value of its momentum. The interaction between each of the quarks and the gluon is represented by an attractive linear potential, the strength of which is taken to be proportional to the attractive force produced by color-octet gluon exchange in the appropriate quark-gluon or antiquark-gluon channel. Gluon exchange here produces a weak repulsive quark-antiquark force. This force is lumped with other short-range effects into the undetermined constant in the Hamiltonian.

While our choice of an effective potential is quite arbitrary, it fits naturally within the framework of currently popular ideas about how quark confinement might occur in the colored quark-gluon model. For example, the linear potential might represent a channelization of color flux, such as takes place in lattice gauge models<sup>9</sup> and magnetic-confinement models based on the superconductivity analogy,<sup>10</sup> or it might represent, in a potential model, an effective confinement resulting from field-theoretic vacuum-polarization instabilities.<sup>11</sup> In either case the magnitude of the effect should increase with the attraction of the single-gluon-exchange force (the Born or classical approximation). Also, these considerations make it clear that one should not treat attractive and repulsive interactions symmetrically. Repulsive Coulomb potentials do not produce vacuum-polarization instabilities, and flux tubes do not develop between repelling monopoles in superconductors nor between repelling quarks in the lattice gauge model.

The constant terms in the Hamiltonian include many effects: rest masses of the charmed quarks, short-range singular potentials, and both repulsive and attractive intermediate-range forces (which might be dynamically different). The asymptotic freedom of gauge theories makes the short-range interactions logarithmically less singular than Coulomb potentials. This is presumably the reason that charmonium models require only a small  $r^{-1}$  term in the potential to fit the observed spectrum well.

Our precise rule for choosing effective two-body interaction potentials is the following. We examine the exchange of an octet of gluons between each pair of particles. The coupling at each vertex is  $g$ , the universal Yang-Mills coupling constant, times a generator of SU(3). This is projected onto each two-body color eigenstate to get an effective

interaction strength. That is, each two-body effective potential is proportional to  $g^2$  times an SU(3) crossing-matrix element. These are computed in the Appendix. If the interaction is attractive we include a linear potential in the Hamiltonian proportional to this effective interaction strength. However, if some two-body interaction is repulsive, we do not represent it by a linear potential, but instead assume that its effect can be included in the constant term.

The absolute strength of the effective  $r$  potentials is determined by comparison with the charmonium calculations.<sup>4</sup> The requirement that a quark-antiquark-gluon ( $\underline{3} \otimes \underline{\bar{3}} \otimes \underline{8}$ ) state is a singlet fixes each of the two-body color configurations. The quark and gluon must be in a  $\underline{3}$ , the antiquark and gluon in a  $\underline{\bar{3}}$ , and the quark and antiquark in an  $\underline{8}$ . As is shown in the Appendix, the forces are attractive between the gluon and both the quark and antiquark, but repulsive and weak between the quark and antiquark. Relative to the charmonium potential (the singlet in  $\underline{3} \otimes \underline{\bar{3}}$ ), the attractive forces here are  $\frac{9}{8}$  times stronger. Relative to charmonium the repulsive quark-antiquark potential has strength  $-\frac{1}{8}$ .

The Hamiltonian of our model in the charmed-quark-antiquark center-of-mass frame is

$$H_{\text{eff}} = 2m_q + \vec{p}_q^2/m_q + |\vec{p}_g| + G(|\vec{r}_q - \vec{r}_{\bar{q}}| + |\vec{r}_{\bar{q}} - \vec{r}_g|) + V_0. \quad (1)$$

$m_q$  is the charmed-quark mass, which is also the reduced mass of the two-quark system.  $\vec{r}_q, \vec{r}_{\bar{q}} = -\vec{r}_q$ , and  $\vec{r}_g$  are the quark, antiquark, and gluon coordinates,  $\vec{p}_q$  is the relative quark momentum, and  $\vec{p}_g$  is the gluon momentum. The interaction strength  $G$  is  $g^2$ , the Yang-Mills coupling constant, times a crossing-matrix element (see the Appendix), times a parameter with the dimensions of (mass)<sup>2</sup>. It is  $\frac{9}{8}$  times the charmonium potential strength.

Except for the constant  $V_0$ , the parameters are deduced from the charmonium model.<sup>4</sup> Their numerical values are

$$\begin{aligned} m_q &= m_c = 1.84 \text{ GeV}, \\ G &= 0.30 \text{ GeV}^2. \end{aligned} \quad (2)$$

Besides burying a lot of physics in the constant  $V_0$ , our effective Hamiltonian contains several approximations. The true center of mass differs somewhat from the quark-antiquark center of mass, so the Hamiltonian can only give bound-state masses to  $O(m_q^{-1})$ . This is the same order of accuracy as our nonrelativistic approximation for the charmed-quark kinetic energy. In addition, both the quarks and the gluon are treated as spinless, so we cannot estimate the spin-orbit or spin-

spin splittings. After computing the energies of the ground state and the lowest excited states, we will put back the spins by hand, in order to find how many states occur at each energy level.

The colored quark-gluon model is both gauge and Lorentz invariant, but our effective Hamiltonian lacks these invariances. The reason for this, of course, is that we have made dynamical approximations and have phrased them in a specific frame and gauge. We have neglected the spins of both the quarks and gluons, and treated the quark kinetic energy nonrelativistically. These approximations were made in the quark-antiquark center-of-mass frame. We have sharply distinguished between the gluon particles and the gluon potential, which we treat instantaneously. This separation is appropriate in the radiation gauge. In this non-covariant, frame-dependent gauge, the gluon field is decomposed into a dynamical part describing massless particles and a dependent field describing an instantaneous potential. We must note, however, that we have no *a priori* argument based on the non-Abelian gauge theory that the effective potential is linear. That is an assumption which we have adopted because of its successful application to the charmonium spectrum.

Our crucial assumption is that, in this gauge and frame, there are states which dominantly consist of one quark, one antiquark, and one gluon. While the general premise of our work, that there is a gluonic component to matter, seems necessary, our specific means of describing the gluonic matter in a new assumption.

There will always be mixing with other configurations, for example states with many gluons, and the amount of mixing will depend on both the frame and the gauge. A more precise statement of our crucial assumption is that in our choice of frame and in the radiation gauge the configuration mixing is small.

If this assumption is correct, then although we cannot fix the energy of the lowest state, the splitting between the lowest,  $s$ -wave, levels and excited,  $p$ -wave levels should be given fairly accurately. More importantly, the model should give the quantum numbers and multiplicities of the low-lying quark-antiquark-gluon states. Because of the spin of the gluon, this spectrum is quite rich.

### III. BOUND-STATE QUANTUM NUMBERS

We analyze the quantum numbers of low-lying bound states by a two-stage procedure that corresponds to expanding the Hamiltonian in powers of  $m_q^{-1}$ . Since the charmed quark is quite heavy, and since our effective Hamiltonian is only valid to  $O(m_q^{-1})$ , this procedure retains the full accuracy

of the model.

To  $O(m_q^0)$ , the Hamiltonian is

$$H^{(0)} = |\vec{p}_g| + G(|\vec{r} + \vec{d}| + |\vec{r} - \vec{d}|) + \text{const.} \quad (3)$$

Here and afterwards we use  $\vec{r}$  as the gluon coordinate and  $\vec{d}$  and  $-\vec{d}$  as the quark and antiquark coordinates.

There are two sets of commuting Hermitian operators that commute with  $H^{(0)}$ :

$$L^2, L_x, |\vec{d}|, \vec{d} \cdot \vec{L} = \vec{d} \cdot \vec{L}_r, \quad (4)$$

and

$$\vec{d}, \vec{d} \cdot \vec{L} = \vec{d} \cdot \vec{L}_r. \quad (5)$$

Each set consists of four operators.  $\vec{L}$  is the total angular momentum which acts both on  $\vec{r}$  and  $\vec{d}$ :

$$\vec{L} = \vec{L}_r + \vec{L}_d.$$

Note that  $\vec{d} \cdot \vec{L}$  is odd under parity,  $P$ , so that parity eigenstates will be superpositions of  $\vec{d} \cdot \vec{L}$  eigenstates. Therefore we will later use  $|\vec{d} \cdot \vec{L}|$  and  $P$  as observables instead of  $\vec{d} \cdot \vec{L}$ .

Let us designate the eigenfunctions of  $H^{(0)}$  which diagonalize the set of operators (4) by  $\Psi$  and those which diagonalize the set (5) by  $\Phi$ . We will use the following notation for the eigenvalues:

Observable	$ \vec{d} $	$\vec{d} \cdot \vec{L}$	$L^2$	$L_x$	(6)
Eigenvalue	$d_0$	$\hat{d}_0$	$l(l+1)$	$l_x$	

When  $\hat{d}_0$  points in the  $z$  direction, we write the wave function  $\Phi$  as

$$\Phi_{d_0, \hat{d}_0, \kappa}(\vec{r}, \vec{d}) \equiv \psi_{d_0, \kappa}(\vec{r}) \delta(\vec{d} - d_0) \delta^2(\hat{d} - \hat{z}). \quad (7)$$

We obtain  $\Phi$  for a general  $\vec{d}_0$  by rotating  $\vec{d}_0$  from  $\hat{z}$  to a direction specified by the spherical angles  $\theta$  and  $\phi$  of  $\vec{d}_0$ , using the rotation operator

$$R_{\vec{d}_0} = R(\phi, \theta, 0). \quad (8)$$

The angles  $\phi, \theta, 0$  are the Euler angles, using the

conventions and notation of Gottfried.<sup>12</sup> The resulting wave function  $\Phi$  is

$$\Phi_{d_0, \hat{d}_0, \kappa}(\vec{r}, \vec{d}) = \psi_{d_0, \kappa}(R_{\hat{d}_0}^{-1} \vec{r}) \delta(\vec{d} - d_0) \delta^2(\hat{d} - \hat{d}_0). \quad (9)$$

By construction,  $\Phi$  is an eigenfunction of the operators  $\vec{d}$  and  $\vec{d} \cdot \vec{L}$ .

The wave functions  $\Psi$  which are eigenfunctions of the set of operators (4) can be expanded in terms of the angular momentum eigenfunctions of  $\vec{r}$  and  $\vec{d}$ :

$$\begin{aligned} \Psi_{l, l_x, d_0, \kappa}(\vec{r}, \vec{d}) \\ = \sum_{\substack{l_1 l_2 \\ m_1 m_2}} C_{l_1 l_2 \kappa}^l(\nu, d_0) \langle l l_x | l_1 m_1 l_2 m_2 \rangle \\ \times Y_{m_1}^{l_1}(\hat{r}) Y_{m_2}^{l_2}(\hat{d}) \delta(\vec{d} - d_0). \end{aligned} \quad (10)$$

This expression displays explicitly the fact that  $\Psi$  is an eigenfunction of  $L^2$ ,  $L_x$ , and  $|\vec{d}|$ .

We must now determine  $C_{l_1 l_2 \kappa}^l(\nu, d_0)$  and find the connection between the  $\Phi$  and the  $\Psi$  wave functions. Since either set of wave functions provides a complete set of energy eigenfunctions, each eigenfunction  $\Phi$  must be expressible as a linear combination of  $\Psi$  eigenfunctions with the same energy, and vice versa. Note that there is an independent  $\Phi$  eigenfunction for each value of  $\hat{d}_0$ , while the eigenvalues of  $H^{(0)}$  clearly do not depend on  $\hat{d}_0$ . This means that each of the energy levels of  $H^{(0)}$  is infinitely degenerate, and each  $\Psi$  eigenfunction is an infinite superposition of  $\Phi$ 's. We represent the connection by

$$\Psi_{l, l_x, d_0, \kappa} = \int d^2 \hat{d}_0 f_{l, l_x, \kappa}(\hat{d}_0) \Phi_{d_0, \hat{d}_0, \kappa}. \quad (11)$$

This relation will determine both  $f_{l, l_x, \kappa}(\hat{d}_0)$  and  $C_{l_1 l_2 \kappa}^l(\nu, d_0)$  in terms of  $\psi_{d_0, \kappa}(\hat{r})$ . We multiply both sides of Eq. (11) by  $Y_{m_1}^{l_1}(\hat{r}) Y_{m_2}^{l_2}(\hat{d})$  and integrate over the angles  $\hat{r}$  and  $\hat{d}$  to obtain

$$C_{l_1 l_2 \kappa}^l(\nu, d_0) \langle l l_x | l_1 m_1 l_2 m_2 \rangle = \int d\hat{d}_0 f_{l, l_x, \kappa}(\hat{d}_0) Y_m^{l_2*}(\hat{d}_0) \int d\hat{r} Y_{m_1}^{l_1*}(\hat{r}) \psi_{d_0, \kappa}(R_{\hat{d}_0}^{-1} \vec{r}). \quad (12)$$

In order to perform the  $\nu$  integration on the right-hand side we make a change of variables and use the rotation property of the spherical harmonics

$$Y_m^l(R\hat{r}) = \sum_{m'} \mathcal{D}_{mm'}^{l*}(R) Y_{m'}^l(\hat{r}). \quad (13)$$

This gives for the  $\hat{r}$  integral

$$\int d\hat{r} Y_{m_1}^{l_1*}(\hat{r}) \psi_{d_0, \kappa}(R_{\hat{d}_0}^{-1} \vec{r}) = \mathcal{D}_{m_1 \kappa}^{l_1}(R_{\hat{d}_0}) e_{d_0, \kappa}^{l_1}(\nu), \quad (14)$$

where

$$e_{d_0, \kappa}^{l_1}(\nu) = \int d\hat{r} Y_{\kappa}^{l_1*}(\hat{r}) \psi_{d_0, \kappa}(\hat{r}). \quad (15)$$

Using the equality

$$Y_m^l(\theta, \phi) = \left(\frac{2l+1}{4\pi}\right)^{1/2} \mathcal{D}_{m0}^{l*}(\phi, \theta, 0), \quad (16)$$

and the definition of  $R_{\hat{d}_0}$  in terms of Euler angles [Eq. (8)], we are led to

$$C_{i_1 i_2 K}^l(\boldsymbol{r}, \boldsymbol{d}_0) \langle l l_z | l_1 m_1 l_2 m_2 \rangle = \int d\hat{d}_0 f_{i_1 i_2 K}(\hat{d}_0) \mathcal{D}_{m_1 K}^{i_1}(\phi, \theta, 0) \mathcal{D}_{m_2 0}^{i_2}(\phi, \theta, 0) \left(\frac{2l_2+1}{4\pi}\right)^{1/2} e_{d_0 K}^{i_1}(\boldsymbol{r}). \quad (17)$$

For this equality to hold one must choose

$$f_{i_1 i_2 K}(\hat{d}_0) = \mathcal{D}_{i_2 K}^{i_1*}(R_{\hat{d}_0}), \quad (18)$$

which, in turn, gives

$$C_{i_1 i_2 K}^l(\boldsymbol{r}, \boldsymbol{d}_0) = \frac{[4\pi(2l_2+1)]^{1/2}}{2l+1} \langle l K | l_1 K l_2 0 \rangle e_{d_0 K}^{i_1}(\boldsymbol{r}). \quad (19)$$

Thus we have expressed  $\Psi$  in terms of  $\psi$ :

$$\Psi_{i_1 i_2 d_0 K}(\vec{\boldsymbol{r}}, \vec{\boldsymbol{d}}) = \mathcal{D}_{i_2 K}^{i_1*}(R_{\hat{\boldsymbol{d}}}) \psi_{d_0 K}(R_{\hat{\boldsymbol{d}}}^{-1} \vec{\boldsymbol{r}}) \delta(d - d_0). \quad (20)$$

We have already remarked that this function is not an eigenfunction of parity,  $P$ .  $H^{(0)}$  commutes with  $P$  and therefore depends only on  $K^2$ , so the two solutions with  $K = \pm|K|$  are degenerate. Parity eigenstates are

$$\Psi_{i_1 i_2 d_0 |K| \eta} = \frac{1}{\sqrt{2}} [\mathcal{D}_{i_2 |K|}^{i_1*}(R_{\hat{\boldsymbol{d}}}) \psi_{d_0 |K|}(R_{\hat{\boldsymbol{d}}}^{-1} \vec{\boldsymbol{r}}) + \eta \mathcal{D}_{i_2 -|K|}^{i_1*}(R_{\hat{\boldsymbol{d}}}) \psi_{d_0 -|K|}(R_{\hat{\boldsymbol{d}}}^{-1} \vec{\boldsymbol{r}})] \delta(d - d_0), \quad (21)$$

where  $\eta = \pm 1$ .

To establish the parity ( $P$ ) and charge-conjugation ( $C$ ) properties of these states we must take into account the spin of the quarks and the  $J^{PC} = 1^{--}$  assignment for the gluon.

Under space reflection,  $\vec{\boldsymbol{r}} \rightarrow -\vec{\boldsymbol{r}}$  and  $\vec{\boldsymbol{d}} \rightarrow -\vec{\boldsymbol{d}}$ , the vector  $R_{\hat{\boldsymbol{d}}}^{-1} \vec{\boldsymbol{r}}$  does not change its length or polar angle, but its azimuthal angle  $\phi$  (about the  $\hat{\boldsymbol{z}}$  axis) becomes  $\pi - \phi$ . The wave function  $\psi_{d_0 K}$  depends on this angle  $\phi$  only through the factor  $e^{iK\phi}$ , so under space reflection

$$\psi_{d_0 K}(R_{\hat{\boldsymbol{d}}}^{-1} \vec{\boldsymbol{r}}) \rightarrow (-1)^K \psi_{d_0 -K}(R_{\hat{\boldsymbol{d}}}^{-1} \vec{\boldsymbol{r}}). \quad (22)$$

Under the change  $\vec{\boldsymbol{d}} \rightarrow -\vec{\boldsymbol{d}}$ , the spherical function becomes

$$\mathcal{D}_{i_2 K}^{i_1}(R_{\hat{\boldsymbol{d}}}) \rightarrow (-1)^i \mathcal{D}_{i_2 -K}^{i_1}(R_{\hat{\boldsymbol{d}}}). \quad (23)$$

Since the intrinsic parity of the quark-antiquark system is  $-1$  and that of the gluon is also  $-1$ , the total parity of the wave function [Eq. (21)] is

$$P = (-1)^{i+K} \eta. \quad (24)$$

Under charge conjugation the quark and antiquark location are exchanged,  $\vec{\boldsymbol{d}} \rightarrow -\vec{\boldsymbol{d}}$ . Under this change both the polar ( $\theta$ ) and azimuthal ( $\phi$ ) angles of  $R_{\hat{\boldsymbol{d}}}^{-1} \vec{\boldsymbol{r}}$  change.

$$\begin{aligned} \theta &\rightarrow \pi - \theta, \\ \phi &\rightarrow -\phi. \end{aligned} \quad (25)$$

If  $\zeta$  denotes the parity of the wave function  $\psi_{d_0 K}$  under the change  $\theta \rightarrow \pi - \theta$ , then under  $C(\vec{\boldsymbol{d}} \rightarrow -\vec{\boldsymbol{d}})$

$$\psi_{d_0 K}(R_{\hat{\boldsymbol{d}}}^{-1} \vec{\boldsymbol{r}}) \rightarrow \zeta \psi_{d_0 -K}(R_{\hat{\boldsymbol{d}}}^{-1} \vec{\boldsymbol{r}}), \quad (26)$$

and, as with space reflection

$$\mathcal{D}_{i_2 K}^{i_1}(R_{\hat{\boldsymbol{d}}}) \rightarrow (-1)^i \mathcal{D}_{i_2 -K}^{i_1}(R_{\hat{\boldsymbol{d}}}). \quad (27)$$

The nonorbital  $C$  of a quark-antiquark system depends on the symmetry of the spin wave function as  $(-1)^{s_{q\bar{q}}}$ , where  $s_{q\bar{q}}$  is the total quark spin. The  $C$  of the gluon is  $-1$ , so under  $C$  the wave function [Eq. (21)] is an eigenfunction of  $C$  with eigenvalue

$$C = (-1)^{i+s_{q\bar{q}}+1} \eta \zeta. \quad (28)$$

It is of course straightforward to express  $P$  and  $C$  in terms of the orbital angular momenta of the gluon  $l_1$ , and the quark,  $l_2$ , relative to the  $q\bar{q}$  center of mass:

$$P = (-1)^{l_1+l_2}, \quad C = (-1)^{l_2+s_{q\bar{q}}+1}. \quad (29)$$

Comparison of Eqs. (24) and (28) with Eq. (29) shows which  $l_1 l_2$  values contribute in Eq. (10) to the formation of a definite  $\Psi$  state. The  $J^{PC}$  quantum numbers of the first few levels are shown in Table I.

So far we have discussed the classification of the eigenfunctions of  $H^{(0)}$ . This corresponds to the limit  $m_q \rightarrow \infty$ . We expressed states with definite angular momentum in terms of the basis  $\Phi$ , which describes states in which the quark and antiquark have a fixed location in space. The infinite degeneracy corresponding to the arbitrariness in the orientation of  $\hat{\boldsymbol{d}}_0$  is lifted to first order in  $m_q^{-1}$  with the introduction of the kinetic energy term

TABLE I. Classification of states.

$ K\rangle$	$\eta$	$\xi$	$l$	$l_{q\bar{q}}$	$l_g$	$s_{q\bar{q}}=0$ $J^{PC}$	$s_{q\bar{q}}=1$ $J^{PC}$
0	+	+	0	0	0	$1^{*-}$	$(0,1,2)^{*-}$
0	+	+	1	1	0	$(0,1,2)^{-*}$	$(0,1,1,1,2,2,3)^{-}$
1	-	+	1	0	1	$(0,1,2)^{-}$	$(0,1,1,1,2,2,3)^{-}$
0	+	-	1				
0	+	-	0	1	1	$1^{*+}$	$(0,1,2)^{*-}$
1	+	+	1	1	1	$(0,1,2)^{*+}$	$(0,1,1,1,2,2,3)^{*-}$
0	+	-	2	1	1	$(1,2,3)^{*+}$	$(0,1,1,2,2,2,3,3,4)^{-}$

for the quarks. Clearly only  $L^2$ ,  $L_x$ , and  $P$  commute with the total Hamiltonian and the eigenfunctions of  $H$  will mix different values of  $d_0$  and  $K$ . The eigenfunction of  $H$  will be of the form

$$\sum_{|K\rangle} \int dd_0 h_{|K\rangle}(d_0) \Psi_{l, l_g, d_0, |K\rangle, \eta} \quad (30)$$

Borrowing terminology from molecular physics we may say that in the limit  $m_q \rightarrow \infty$  all quark rotational levels are degenerate and their vibrational degree of freedom is frozen. To first order in  $m_q^{-1}$  the vibrational as well as rotational degrees of freedom are excited. In contradistinction to atoms in molecules, the quarks do not sit in a potential well and therefore the vibrational splittings can be expected to be of the same order as the rotational ones. It remains to be seen how they compare with the "electronic level" splittings, the differences of energy eigenvalues of  $H^{(0)}$ . This calls for a numerical evaluation which will be done in the next section.

#### IV. THE BOUND-STATE SPECTRUM

In this chapter we will make variational numerical estimates of the lowest-energy states in the  $q\bar{q}g$  spectrum. We limit ourselves to the case of charmed quarks, so we can use the  $m_q^{-1}$  expansion.

The first question that confronts us is the choice of a variational trial function. The potential energy in Eqs. (1) and (3) can be diagonalized in prolate spheroidal coordinates, since the equipotential surfaces are ellipsoids whose two foci are the locations of the two quarks. This suggests using gluon trial wave functions which are constant on the equipotential surfaces. The family of such ellipsoids is defined by a continuous parameter  $\nu$ , where

$$|\vec{r} + \vec{d}| + |\vec{r} - \vec{d}| = 2d \cosh \nu. \quad (31)$$

The two other variables which define this coordinate system are an angle  $\alpha$  given by

$$|\vec{r} + \vec{d}| - |\vec{r} - \vec{d}| = 2d \cos \alpha \quad (32)$$

and the azimuthal angle  $\phi$ . The gluon momentum operator is of course somewhat complicated in this coordinate system. An alternative choice is a spherically symmetrical trial function for the gluon.

We carried out variational calculations using both types of trial functions. We obtained somewhat lower energies for spherically symmetrical ground-state trial wave functions. The reason is that the trial functions of the form  $e^{-\lambda (\cosh \nu - 1)}$ , which are constant on the equipotential ellipsoids and which we used as a ground-state trial function, include high angular momentum components in the region where  $|\vec{r}|$  is of the same order of magnitude as  $|\vec{d}|$ . Using the  $m_c$  value of Eq. (2), the angular momentum degeneracy is fairly strongly broken, thus favoring s waves in both quark and gluon coordinates. It is therefore the  $m_c^{-1}$  term, the quark kinetic energy, which leads us to prefer spherically symmetrical trial functions.

We estimate the ground-state energy by using normalized trial states of the form

$$\Psi_0 = \frac{(\lambda \mu)^{3/2}}{8\pi} e^{-(\lambda/2)r} e^{-(\mu/2)d}. \quad (33)$$

We vary

$$\omega_0 = \langle \Psi_0 | H | \Psi_0 \rangle \quad (34)$$

with respect to both  $\mu$  and  $\lambda$ , and find the smallest value. A straightforward calculation leads to

$$\begin{aligned} \omega_0 = & \frac{4\lambda}{3\pi} + 2G \left( \frac{3(\mu + \lambda)}{\mu\lambda} - \frac{3}{\mu + \lambda} - \frac{\lambda\mu}{(\lambda + \mu)^3} \right) \\ & + \frac{\mu^2}{16m_c} + 2m_c + V_0. \end{aligned} \quad (35)$$

The first term is the gluon kinetic energy, the second is the expectation value of the linear potential, and the third is the quark kinetic energy. Using the values of the parameters [Eq. (2)] one finds the minimal value for  $\lambda = 1.9$  GeV,  $\mu = 2.6$  GeV. It is (in GeV)

$$\begin{aligned} \omega_0 = & 0.81 + 1.20 + 0.23 + 2m_c + V_0 \\ = & 2.23 + 2m_c + V_0. \end{aligned} \quad (36)$$

The contribution of each term in Eq. (35) is shown explicitly.

A similar calculation can now be carried out for the excited state which has  $l_q = 1$ :

$$\psi_1 = \frac{\lambda^{3/2} \mu^{5/2}}{8\sqrt{3}\pi} e^{-\lambda r/2} d Y_1^1(\vec{d}) e^{-\mu d/2}. \quad (37)$$

The minimal value is obtained for  $\lambda = 1.8$  GeV,  $\mu = 3.1$  GeV, and is

$$\begin{aligned} \omega_1 = & 0.76 + 1.40 + 0.33 + 2m_c + V_0 \\ = & 2.50 + 2m_c + V_0. \end{aligned} \quad (38)$$

The gluon  $p$ -wave function will be described by

$$\psi_2 = \frac{\lambda^{5/2} \mu^{3/2}}{8\sqrt{3}\pi} r Y_m^1(\hat{r}) e^{-\lambda r/2} e^{-\mu d/2} . \quad (39)$$

Its minimal energy is obtained for  $\lambda = 2.3$  GeV,  $\mu = 2.4$  GeV, and is

$$\begin{aligned} \omega_2 &= 1.17 + 1.51 + 0.20 + 2m_c + V_0 \\ &= 2.88 + 2m_c + V_0 . \end{aligned} \quad (40)$$

At this point we can quantitatively examine the molecular analogy of the preceding chapter. The gluon  $p$  wave is the analog of an excited electronic level. Although its excitation energy is greater than that of the quark  $p$  wave, the analog of a molecular rotational excitation, it is of the same order of magnitude. This rough equality depends on the relative values of the various parameters in our calculations. Only if  $m_q$  were an order-of-magnitude larger would one find an order-of-magnitude difference between gluon and quark rotational excitations.

From these numerical results we infer the likely structure of the low-mass  $c\bar{c}g$  bound-state spectrum. Small variations of the parameters used in our calculation do not change the qualitative conclusions.

The ground state should be mostly  $s$  wave in both quarks and gluon. The quantum numbers of the corresponding particle states are

$$J^{PC} = 0^{++}, 1^{++}, 2^{++}, 1^{+-} , \quad (41)$$

taking into account the spins of the quarks and gluon. This spectrum is the same as that of a  $p$ -wave  $c\bar{c}$  system. Indeed one should expect that physical states are an admixture of these two different types of bound states. A few hundred MeV higher, about the same as the separation between the  $J/\psi(3.1)$  and the  $\chi$  states, one expects the second level of particle states, whose wave functions primarily describe  $p$ -wave quarks and an  $s$ -wave gluon. This level contains many particle states (see Table I):

$$J^{PC} = (0, 1, 2)^{-+} \text{ and } (0, 1, 1, 1, 2, 2, 3)^{--} . \quad (42)$$

The two groupings in Eq. (42) correspond to  $s_{q\bar{q}} = 0$  and 1, respectively. Here we find for the first

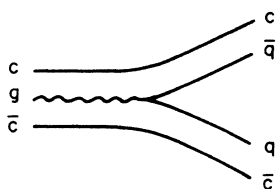


FIG. 1. The dominant decay amplitude for low-mass  $c\bar{c}g$  states, those below the  $c\bar{q}g \oplus q\bar{c}$  threshold.

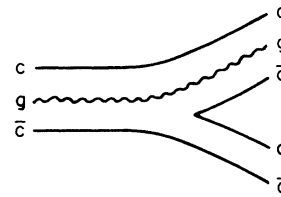


FIG. 2. The dominant two-body decay amplitude for high-mass  $c\bar{c}g$  states.

time states whose quantum numbers are such that they cannot be made from a quark and antiquark alone ("exotics of the second kind"). These are the  $1^{-+}$  and  $0^{--}$  states. These states are forbidden from decaying into  $N\bar{N}$ . In addition, there are three ordinary vector mesons. Although their coupling to the photon is allowed only through admixture with  $c\bar{c}$  states,<sup>8</sup> these may be some of the many close resonances seen in  $e^+e^-$  annihilation.

The next level of states should occur another several hundred MeV higher and include the states with  $l_g = 1, l_q = 0$ . These states will have the opposite charge conjugation as the  $l_g = 0, l_q = 1$  states (see Table I). They also include states which are exotics of the second kind, i.e., which cannot decay into  $N\bar{N}$ . The prediction of exotic states as well as the multitude of new vector mesons is exciting. One would like to know at what mass these states will begin.

The answer depends on the value of  $V_0$ . In charmonium calculations with the same parameters that we have used,  $V_0$  is determined by the observed  $J/\psi$  mass to be  $-1.37$  GeV. To the extent that  $V_0$  represents the short-range Coulomb term, one could expect it to be roughly twice as big in our calculation. That would bring the ground state of our calculation down to near the  $J/\psi$  mass. However, another component of  $V_0$  stems from repulsion from the continuum of charmed states.<sup>4</sup> This effect could be much weaker for  $c\bar{c}g$  states. Using the magnitude of  $V_0$  in the charmonium calculation as a measure of the ignorance covered up by this term, we can make an "educated guess" that the ground state of  $c\bar{c}g$  lies somewhere between the  $J/\psi$  and 2 GeV above. Wherever it lies, we expect that the first excited quark rotational level is only about 300 MeV higher, and the first gluon rotational excitation a similar amount above that.

Let us close this section with a short discussion of how the  $c\bar{c}g$  states can be expected to decay. We propose the process shown in Fig. 1 as the decay vertex for the low-lying states; i.e., we assume that the decay proceeds by the conversion of the gluon into a  $q\bar{q}$  pair. An alternative mechanism is the one shown in Fig. 2, in which there is also a

$c\bar{c}g$  state in the outgoing channel. For high-mass resonances one would expect the Fig. 2 process to dominate, since it does not involve the  $gq\bar{q}$  vertex. However, for low-lying  $c\bar{c}g$  states it seems likely that the  $c\bar{q} \oplus \bar{c}q$  channel will be open while the  $cg\bar{q} \oplus \bar{c}q$  one will still be below its threshold, thus allowing only the Fig. 1 process. An example of the consequences of this assumption is that there is one linear combination of the three  $1^{--}$  states of Eq. (42) that can decay into  $D^*\bar{D}^*$  but not into  $D\bar{D}^*$  or  $D\bar{D}$ . That state corresponds to the  $c\bar{c}$  and gluon spins being combined into an overall spin 2. It can decay via Fig. 1 only into two mesons, each of total constituent spin 1. Straightforward spin rearrangement calculations show that of the other two linear combinations of  $1^{--}$  states, only that with total spin 0 can decay into  $D^*\bar{D}^*$ , and its decay amplitude will be only  $\frac{1}{2}$  as strong as that of the total spin-2 combination. This example is of interest because the 4.028-GeV resonance in  $e^+e^-$  annihilation seems to have an anomalously large decay rate into  $D^*\bar{D}^*$ , a fact which has recently led De Rujula *et al.*<sup>13</sup> to propose that this state is a  $D^*\bar{D}^*$  molecule. In our model we could associate this resonance with a  $1^{--}$  state that has a large admixture of the constituent spin-2 state discussed above.

## V. DISCUSSION AND SUMMARY

The features of the spectrum of hadrons can be successfully described in terms of a simple quark-model picture. In particular one of the impressive qualitative conclusions of low-mass phenomenology is the absence of exotic states, i.e., mesons and baryons that cannot be constructed from  $q\bar{q}$  and  $qqq$  combinations. Although confinement in a color-SU(3) gauge theory would explain the absence of colored hadrons,<sup>9,10,11</sup> it would still be possible that exotic color-singlet states exist. In fact it should be expected that the spectrum of a field-theoretical model will be more complicated than that of an effective-potential model with a fixed number of constituents.

The details of the spectrum of the low-mass hadrons become unclear above the 2-GeV region. Thus one rarely observes radial excitations of meson families. It seems likely, therefore, that if exotics exist they will more readily be found in an experimental study of particles composed out of heavy (charmed) quarks. There, a two-year experimental program led to a harvest of five states in the same  $J^{PC} = 1^{--}$  channel.

From a theoretical point of view, heavy quarks are also a blessing; they justify an  $m_q^{-1}$  expansion, i.e., nonrelativistic calculations. We made use of this fact in our model by introducing an ef-

fective Hamiltonian to calculate a specific family of new states. Spectroscopic predictions of particles constructed from charmed quarks<sup>14</sup> have turned out to be very successful.<sup>15</sup> The meaning of the mass of a quark seems to be better understood nowadays in the light of asymptotically free gauge theories.<sup>16</sup> Nevertheless it is still unclear how the field theory generates the relatively simple potential structures used in charmonium<sup>3,4</sup> and the present calculations.

In our model we introduced an extra ingredient to the well-established constituent quarks—a constituent massless gluon. The gluon field plays an important role in the formulation of quantum chromodynamics, and it seems to us reasonable to assume that it should play an important role as a spectroscopic constituent also, in addition to being the carrier of the confining forces. The proof of this approach should lie, as in the case of constituent quarks, in experimental spectroscopic verifications.

We mentioned in the Introduction the question of gauge invariance that is naturally associated with the concept of the gluon. Our calculation is done within a specific gauge. In this framework one can clearly envisage many other exotic systems, for example, those gotten by adding more gluons or light quark-antiquark pairs. It remains to be seen if any exotic structure will be found, and, in case it is found, if it follows the hierarchy of states outlined in the preceding section.

The main qualitative prediction of our calculation is the small splitting between the ground and excited levels. The first 300-MeV splitting between the  $s$  and  $p$  waves of the charmed-quark-antiquark pair is a feature determined by their large mass. This should be invariant under small changes in the other parameters of our model. We expect that even if the gluon acquires a small mass by some dynamical spontaneous symmetry breaking,<sup>17</sup> since the gluon has high momentum (see Sec. IV), it should not lead to qualitative changes. As a matter of fact, we also applied our model to doubly charmed baryons, and found there too a characteristic mass splitting of about 300 MeV for the first excitation of the angular momentum of the charmed-quark pair.

Finally, one should emphasize the large number of states resulting from our model. In particular, there is an abundance of vector mesons in the first excited levels. These new states may account for one or more of the excitations observed in  $e^+e^-$  annihilation. Although the general features of the observed resonance structure may be explained by the charmonium model,<sup>18</sup> there are experimental puzzles that may require states of the new kind (see discussion at the end of Sec. IV). If this is



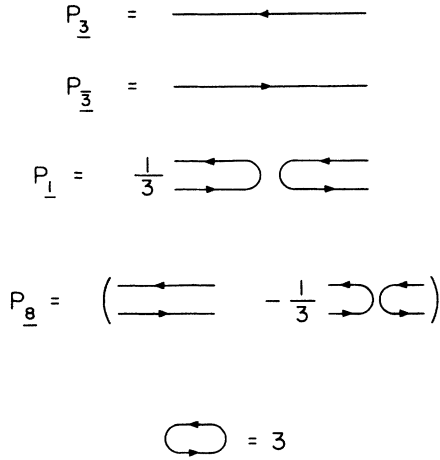


FIG. 3. Diagrammatic representations of the projection operators on the  $\underline{3}$ ,  $\overline{3}$ ,  $\underline{8}$ , and  $\underline{1}$  representations and of the trace formula  $\text{Tr } P_{\underline{3}} = 3$ .

true then all our other states (see Table I) should also be found in the same region, which means that further experimental studies should reveal a rich spectroscopic treasure.

APPENDIX

In this Appendix we compute the strength of the potential resulting from octet exchange. In our model, the effective potential is linear but its strength is assumed to be proportional to the potential produced by octet gluon exchange, with the gluon having universal gauge couplings to each kind of particle, quarks or gluons. The effective strength of the octet exchange potential depends on the direct channel. The numbers that express the relative strengths are SU(3) crossing-matrix elements.

We compute these numbers using diagrams.<sup>19</sup> Lines in the diagrams represent particles with given quantum numbers, or, more abstractly, projection operators on their representations.

Figure 3 shows the diagrams representing the projection operators on the  $\underline{3}$  and  $\overline{3}$  representations in the quark and antiquark sectors, and on the  $\underline{8}$  and  $\underline{1}$  representations on the  $q\bar{q}$  sector. A closed loop stands for the number of basis elements (quarks) of the  $\underline{3}$  representation, i.e., the number 3. The reader may verify that these are the proper diagrams by checking that, within each sector,

$$P_i P_j = P_i \delta_{ij}, \tag{A1}$$

and that the trace of each  $P$  (computed by joining each line position end-to-end and using the rule that a closed loop equals 3) is the indicated dimension.

The vertex coupling an exchanged gluon to either  $\underline{3}$ ,  $\overline{3}$ , or  $\underline{8}$  is shown in Fig. 4. The pair of oppositely directed lines coming from the bottom of each diagram represents a double-index, traceless tensor labeling of the generators,  $G^{ij}$ , of SU(3). The indices  $i$  and  $j$  run from 1 to 3, but there are only eight independent generators since  $\sum_i G^{ii} = 0$ . The connection with the conventional labeling<sup>20</sup> is that

$$G^{ij} = \frac{1}{\sqrt{2}} \sum_{a=1}^8 (\lambda^a)_{ij} G_a, \tag{A2}$$

$$G_a = \frac{1}{\sqrt{2}} \sum_{i,j} (\lambda^a)_{ij} G^{ij},$$

where

$$[G_a, G_b] = i \sum_c f_{abc} G_c. \tag{A3}$$

The numerical factors are chosen so that

$$\begin{aligned} \text{Tr } G_{\underline{3}}^{ij} G_{\underline{3}}^{i'j'} &= \frac{1}{2} P_{\underline{8}}^{ij, i'j'} \\ &= \frac{1}{2} (\delta^{ij'} \delta^{i'j} - \frac{1}{3} \delta^{ij} \delta^{i'j'}). \end{aligned} \tag{A4}$$

$P_{\underline{8}}$  is the normalized octet projection symbolized in Fig. 3. This corresponds to the conventional normalization for the  $\lambda$  matrices,

$$\text{Tr} (\frac{1}{2} \lambda_a) (\frac{1}{2} \lambda_b) = \frac{1}{2} \delta_{ab}. \tag{A5}$$

As the diagrams show, the  $G_{\overline{3}}$  matrices are the negative transposes of the  $G_{\underline{3}}$  matrices. Since the  $\underline{8}$  is the only nontrivial representation contained in  $\overline{3} \otimes \underline{3}$  ( $G_{\underline{1}}^{ij} = 0$ ), the octet generators are obtained by the direct product formula

$$G_{\underline{8}} = I_{\overline{3}} \otimes G_{\underline{3}} + G_{\overline{3}} \otimes I_{\underline{3}}. \tag{A6}$$

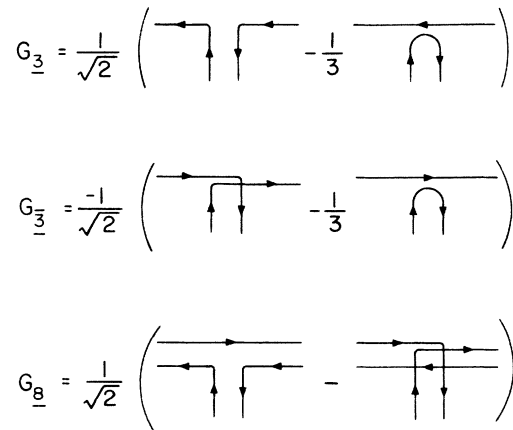


FIG. 4. Diagrammatic representations of the vertices coupling an SU(3) generator to the  $\underline{3}$ ,  $\overline{3}$ , and  $\underline{8}$  representation, that is, representations of these matrix elements of the generators.

$$\begin{aligned}
 A^{(\bar{3},3)} &= -\frac{g^2}{2} \left( \text{diagram 1} - \frac{1}{3} \text{diagram 2} \right) \\
 &= \frac{g^2}{6} \left( \text{diagram 3} - \frac{1}{3} \text{diagram 4} \right) \\
 &\quad - \frac{4}{3} g^2 \left( \frac{1}{3} \text{diagram 5} \right) \\
 &= \frac{g^2}{6} P_{\underline{8}} - \frac{4}{3} g^2 P_{\underline{1}}
 \end{aligned}$$

FIG. 5. Decomposition of the octet-exchange amplitude for  $\bar{3} \otimes 3 \rightarrow \bar{3} \otimes 3$  into direct-channel amplitudes.

Figure 5 is a diagrammatic representation of the amplitude for octet exchange between a  $\bar{3}$  and a  $3$ . By rearranging the lines and adding and subtracting diagrams, the amplitude is decomposed into

$$\begin{aligned}
 P_{\underline{15}}^{(8 \otimes 3)} &= \frac{1}{2} \left( \text{diagram 1} + \text{diagram 2} \right) \\
 &\quad - \frac{1}{8} \left( \text{diagram 3} + \text{diagram 4} \right. \\
 &\quad \left. + \text{diagram 5} + \text{diagram 6} \right) \\
 P_{\underline{6}}^{(8 \otimes 3)} &= \frac{1}{2} \left( \text{diagram 1} - \text{diagram 2} \right) \\
 &\quad - \frac{1}{4} \left( \text{diagram 3} + \text{diagram 4} \right. \\
 &\quad \left. - \text{diagram 5} - \text{diagram 6} \right) \\
 P_{\underline{3}}^{(8 \otimes 3)} &= \frac{3}{8} \text{diagram 3} + \frac{1}{24} \text{diagram 4} \\
 &\quad - \frac{1}{8} \text{diagram 5} - \frac{1}{8} \text{diagram 6}
 \end{aligned}$$

FIG. 6. Diagrammatic representations of the projection operators on the  $\underline{15}$ ,  $\underline{6}$ , and  $\underline{3}$  representations in the  $\underline{8} \otimes \underline{3}$  sector.

$$\begin{aligned}
 A^{(8,3)} &= -\frac{g^2}{2} \left( \text{diagram 1} - \text{diagram 2} \right) \\
 &= \frac{g^2}{2} P_{\underline{15}}^{(8 \otimes 3)} - \frac{g^2}{2} P_{\underline{6}}^{(8 \otimes 3)} - \frac{3}{2} g^2 P_{\underline{3}}^{(8 \otimes 3)}
 \end{aligned}$$

FIG. 7. Decomposition of the octet-exchange amplitude for  $\underline{8} \otimes \underline{3} \rightarrow \underline{8} \otimes \underline{3}$  into direct-channel amplitudes.

direct-channel amplitudes. The coefficient multiplying each direct-channel projection operator is the strength of the effective potential in that channel. Thus we see that in the singlet channel there is an attractive (negative) potential of strength  $-\frac{4}{3}g^2$ , while in the octet representation there is a repulsive (positive) potential of strength  $\frac{1}{6}g^2$ .

Figure 6 shows the diagrams representing projection operators on each of the representations contained in  $\underline{8} \otimes \underline{3}$ , namely  $\underline{15}$ ,  $\underline{6}$ , and  $\underline{3}$ . As with Fig. 3, the reader may verify that these are the proper diagrams by checking that each satisfies  $P^2 = P$ , that the product of any pair vanishes, and that the trace of each is, in fact, the dimension of the representation.

Figure 7 is a diagram representing the octet exchange amplitude between an  $\underline{8}$  and a  $\underline{3}$ . Again, by rearrangement, addition and subtraction of diagrams, the amplitude can be drawn to show its direct-channel structure. The result is that there is a repulsive potential of strength  $\frac{1}{2}g^2$  in the  $\underline{15}$  channel, and attractive potentials of strength  $-\frac{1}{2}g^2$  in the  $\underline{6}$  channel and  $-\frac{3}{2}g^2$  in the  $\underline{3}$  channel.

The entire calculation symbolized by Figs. 6 and 7 can be adapted to find potential strengths in the representations contained in  $\underline{8} \otimes \underline{3}$ . Diagrammatically this is most simply accomplished by changing the sense of every arrow in these diagrams. This operation preserves all algebraic relations between diagrams: the commutation and trace relations used to identify generators, the product and trace relations used to identify projection operators, and the arithmetic connections between diagrams used to evaluate the potential strengths in each channel. Hence octet exchange between  $\underline{8}$  and  $\bar{3}$  leads to a repulsive potential of strength  $\frac{1}{2}g^2$  in the  $\underline{15}$  channel and attractive potentials of strengths  $-\frac{1}{2}g^2$  in the  $\underline{6}$  channel and  $-\frac{3}{2}g^2$  in the  $\underline{3}$  channel.

Thus relative to the attractive effective potential in the singlet channel of  $\bar{3} \otimes \underline{3}$ , there is an attractive potential  $\frac{3}{8}$  times as strong in the  $\underline{3}$  channel of  $\underline{8} \otimes \underline{3}$  and in the  $\bar{3}$  channel of  $\underline{8} \otimes \bar{3}$ , and a repulsive potential  $\frac{1}{8}$  as strong in the  $\underline{8}$  channel of  $\bar{3} \otimes \underline{3}$ .

- \*Work supported in part by the U. S. Energy Research and Development Administration under Contract No. E(11-1)-68.
- †On leave of absence from Tel-Aviv University, Tel-Aviv, Israel.
- ‡Work supported in part by the Alfred P. Sloan Foundation and in part by the National Science Foundation under Grant No. PHY7612396.
- <sup>1</sup>Review is given by H. D. Politzer, *Phys. Rep.* 14, 129 (1974).
- <sup>2</sup>Review is given by F. J. Gilman, rapporteur talk, in *Proceedings of the XVII International Conference on High Energy Physics, London, 1974*, edited by J. R. Smith (Rutherford Laboratory, Chilton, Didcot, Berkshire, England, 1974), p. IV-149.
- <sup>3</sup>T. Appelquist and H. D. Politzer, *Phys. Rev. Lett.* 34, 43 (1975); and *Phys. Rev. D* 5, 1404 (1975).
- <sup>4</sup>E. Eichten *et al.*, *Phys. Rev. Lett.* 34, 369 (1975); 36, 500 (1976).
- <sup>5</sup>J. L. Rosner, *Phys. Rev. Lett.* 21, 950 (1968); 21, E1468 (1968); K. Johnson and C. B. Thorn, *Phys. Rev. D* 13, 1934 (1976); R. Jaffe, *ibid.* 15, 267 (1977); 15, 281 (1977); M. Bander, G. L. Shaw, P. Thomas, and S. Meshkov, *Phys. Rev. Lett.* 36, 695 (1976); C. Rosenzweig, *ibid.* 36, 697 (1976); N.-P. Chang and C. A. Nelson, *Phys. Rev. D* 15, 1412 (1977).
- <sup>6</sup>R. P. Feynman, *Photon-Hadron Interactions* (Benjamin, Reading, Mass., 1972).
- <sup>7</sup>Review is given by E. S. Abers and B. W. Lee, *Phys. Rep.* 9C, 1 (1973).
- <sup>8</sup>Y. Dothan and D. Horn, *Nucl. Phys.* B114, 400 (1976).
- <sup>9</sup>K. Wilson, *Phys. Rev. D* 10, 2445 (1974); J. Kogut and L. Susskind, *ibid.* 11, 395 (1975).
- <sup>10</sup>H. P. Nielsen and P. Olesen, *Nucl. Phys.* B61, 45 (1973); Y. Nambu, *Phys. Rev. D* 10, 4262 (1974); S. Mandelstam, *Phys. Lett.* 53B, 476 (1975).
- <sup>11</sup>A. Casher, J. Kogut, and L. Susskind, *Phys. Rev. Lett.* 31, 892 (1973); and *Phys. Rev. D* 10, 732 (1974); J. Mandula, *Phys. Lett.* 76B, 175 (1977).
- <sup>12</sup>K. Gottfried, *Quantum Mechanics I* (Benjamin, Reading, Mass., 1966).
- <sup>13</sup>A. De Rújula, H. Georgi, and S. L. Glashow, *Phys. Rev. Lett.* 38, 317 (1977).
- <sup>14</sup>A. De Rújula, H. Georgi, and S. L. Glashow, *Phys. Rev. D* 12, 147 (1975).
- <sup>15</sup>G. Goldhaber *et al.*, *Phys. Rev. Lett.* 37, 255 (1976); I. Peruzzi *et al.*, *ibid.* 37, 569 (1976); B. Knapp *et al.*, *ibid.* 37, 882 (1976).
- <sup>16</sup>H. Georgi and H. D. Politzer, *Phys. Rev. D* 14, 1829 (1976).
- <sup>17</sup>W. A. Bardeen and R. B. Pearson, *Phys. Rev. D* 14, 547 (1974).
- <sup>18</sup>K. Lane and E. Eichten, *Phys. Rev. Lett.* 37, 477 (1976).
- <sup>19</sup>J. Mandula, in preparation.
- <sup>20</sup>M. Gell-Mann, *Phys. Rev.* 125, 1067 (1962).